AN INTEGRATED GPS/INS/BARO AND RADAR ALTIMETER SYSTEM FOR AIRCRAFT PRECISION APPROACH LANDINGS

Robert A. Gray and Peter S. Maybeck

Department of Electrical and Computer Engineering
Air Force Institute of Technology
Wright-Patterson AFB, OH 45433

1. Abstract

Currently, the Department of Defense (DOD) and the commercial airline industry are utilizing the Instrument Landing System (ILS) during aircraft landings for precision approaches. The replacement system for the aging ILS was thought to be the Microwave Landing System (MLS). Instead, use of the Global Positioning System (GPS) is now thought to be a viable replacement for ILS precision approaches. The majority of current precision landing research has exploited "stand-alone" GPS receiver techniques. This paper instead explores the possibilities of using an extended Kalman filter (EKF) that integrates an Inertial Navigation System (INS), GPS, Barometric Altimeter, Pseudolite and Radar Altimeter for aircraft precision approaches. This paper shows that integrating the INS, GPS, Barometric Altimeter and Radar Altimeter meets Federal Aviation Administration (FAA) requirements for a Category I precision approach, and additionally integrating a single Pseudolite meets FAA requirements for a Category II precision approach.

2. Introduction

This paper concentrates on setting up reliable models for a high (0.4 nm/hr CEP), medium (2 nm/hr CEP) and low accuracy INS (4 nm/hr CEP) to cover the range of accuracies from DoD and airline systems to cheaper systems for civil aviation, GPS (5 channel receiver, 5m vertical and 4m horizontal precision, 1σ), Baro Altimeter (50 - 150ft, 1σ), and Radar altimeter (1% of altitude +1ft, 1σ). This research also develops a generic precision approach flight profile (using PROFGEN [30]) that encompasses a majority of aircraft types. Lastly, this paper utilizes a single ground-based SV (pseudolite) and available true post-processed ephemeris data [6], instead of computer-simulated orbit functions [2,16,29,32,36]. Once all the above elements are in place, the Multimode Simulation for Optimal Filter Evaluation (MSOFE) [31] is utilized to perform extended Kalman Filter integration analysis.

3. Assumptions

This section outlines the assumptions that have been made in this paper.

1. All work has been conducted through computer simulation. The "real" world in the simulation is modeled as a full-order truth error-state model. The full-order truth and filter models are presented in Section 6.
2. The INS platform is assumed to be stabilized with a barometric (baro) altimeter. An INS platform is unstable without an outside measurement source in the vertical channel [4]. While a baro altimeter is not the only way to stabilize a platform, it is a commonly used method. The use of the baro altimeter is included in the modeling of the system. The majority of commercial and military aircraft utilize a radar altimeter in a stand-alone mode for terminal approaches to a runway. This paper will instead exploit the radar altimeter as an independent measurement device feeding an extended Kalman filter. The radar altimeter measurements will be utilized at altitudes below 3000 feet above ground level (AGL). In summary, this paper will use both the barometric *and* radar altimeter measurements.
3. A sample period of one second has been chosen (unless otherwise noted) for the EKF. The sample period refers to how often the GPS and radar altimeter measurements will be brought into the EKF. Past AFIT research has used a variety of sample periods, varying from two to ten seconds [29,32]. The decision to use one second sample period is based primarily on the typical availability of the GPS measurement in the real world. Though the author is aware of a few GPS receivers which output measurements at a rate of ten times a second (10 Hz), a one second sample period is chosen as a good, representative design choice.
4. The computer simulations have been developed using a program called Multi-mode Simulation for Optimal Filter Evaluation (MSOFE) [31]. MSOFE is well-established Air Force software to develop and test Kalman filter algorithms.
5. The computer-simulated flight profile has been generated by the program PROFGEN [30]. PROFGEN is designed to work with MSOFE to provide the necessary data files to simulate dynamic flight profiles.
6. The plotted outputs are generated by the commercial software package MATLAB [38].
7. The SV ephemeris data using System Effectiveness Model (SEM) [10] software was obtained from the Coast Guard BBS. The ephemeris data is post-processed by the U.S. Department of Commerce, National Geodetic Information Branch [6].
8. The four SVs chosen to range during operation of MSOFE and the FLIGHT profile are chosen based on the indicated results of the System Effectiveness Model (SEM3.6) software from [10] based on position dilution of position (PDOP).
9. The simulation software, MSOFE and MATLAB, has been coded to run in double precision to increase the numerical stability and precision of the simulation. MSOFE software utilizes a U-D factorization algorithm to increase the numerical stability in the Kalman filter measurement update equations [26,31].
10. The MSOFE runs are conducted using 15-run Monte Carlo analyses. While a larger batch size for the Monte Carlo analysis would be preferable, this value has been chosen to keep the computational burden within reasonable bounds, while maintaining

adequate confidence that the resulting sample statistics properly reflect the true underlying statistics.

11. It will be assumed for this paper that, when radar altimeter measurements are available, the earth's surface will be modeled as flat and referenced approximately to the INS-indicated altitude (referenced to WGS-84 ellipsoid). This assumption will definitely have to be "upgraded" to a more realistic radar altimeter scenario at a later time by possibly using a database that contains "height of terrain" for specific locations on the earth.
12. The INS will have had a "normal" 8-minute alignment and nominal flight of sixty (60) minute duration prior to the terminal approach phase under investigation.
13. Four SV are always available, with an average PDOP of 2.
14. The transport aircraft flight profile will:
    a. Always be at less than 0.9g during entire flight.
    b. Have a takeoff speed of 150 knots.
    c. Have a landing speed of 133 knots at a 3 degree glideslope.
    d. Maintain airspeed greater than 250 knots above 10,000 ft altitude.
    e. Change altitude at a rate 4000 ft/min (maximum).
    f. Follow the approach plate of [7].

4. Key Terms and Definitions

Ring Laser Gyro (RLG) Strapdown INS: By definition [21], an *inertial navigator* is a self-contained, dead-reckoning navigation aid using inertial sensors, a reference direction, and initial or subsequent fixes to determine direction, distance, and speed; single integration of acceleration provides speed information and a double integration provides distance information.

The strapdown system is mechanized by mounting three gyros and three accelerometers directly to the vehicles for which the navigation function is to be provided. An onboard digital computer keeps track of the vehicle's attitude with respect to some reference frame based on information from the gyros. The computer is thus able to provide the coordinate transformation necessary to coordinatize the accelerometer outputs in a computational reference frame.

RLG construction typically consists primarily of an optical cavity, a laser device, three or four mirrors, a prism, and a pair of photo detectors [34,36]. The RLG operates as follows [18,34,36]: the laser gyro detects and measures angular rates by measuring the frequency difference between two contra-rotating (laser) beams. The two laser beams circulate in the "ring" cavity simultaneously. If the cavity is rotating in an inertial sense, the propagation times of the two light beams are different. The delay manifests itself in the form of a phase shift between the two beams, and the phase shift is detected by a pair of photo detectors [34,36]. Devices of this type are extremely reliable due to the absence of moving parts [34,36].

Specific force is measured by accelerometers. The most common accelerometers to date have been devices which are sophisticated variations of the simple pendulum [4,36]. To obtain the correct measure of inertial acceleration, the effects of local gravity must be removed from the measured specific force [4,33].

Barometric Altimeter: A shortcoming of any INS is the instability present in the vertical channel which (in the absence of aiding information) results in unbounded error growth in vertical position and velocity [2,4,14,33]. This inherent instability is controlled by vertical channel aiding. Such aiding is frequently accomplished in vertical position information provided from a barometric altimeter. This external altitude information has the effect of stabilizing the vertical channel [4]. Barometric altimeters are most inaccurate when ascending or descending at rapid rates (especially noted with fighter aircraft) but are relatively low cost.

Global Positioning System (GPS): GPS navigation presents opportunity for standardized worldwide civil aviation operations using a common navigation receiver [12]. GPS is a space-based positioning, velocity and time system that has three major segments: Space, Control and User.

GPS Space Segment: The GPS *Space* Segment is composed of 24 satellites in six orbital planes. The satellites operate in near-circular 20,200 km (10,900 NM) orbits at an inclination angle of 55 degrees and with ≈12-hour period. The spacing of satellites in orbit is arranged so that a minimum of five satellites will be in view to users worldwide, with a position dilution of precision (PDOP) of six or less. PDOP is a measure of the error contributed by the geometric relationships of the GPS satellites as seen by the GPS receiver [9]. PDOP is mathematically defined as:

$$PDOP = (\sigma_x^2 + \sigma_y^2 + \sigma_z^2)^{1/2}$$

where σ_x^2, σ_y^2 and σ_z^2 are the variances of the x, y and z pseudorange measurement position errors [9]. Each satellite transmits on two L band frequencies, L1 (1575.42 MHz) and L2 (1227.6 MHz). L1 carries a precise (P) code and a coarse/acquisition (C/A) code. L2 carries the P code. A navigation data message is superimposed on these codes. The same navigation data message is carried on both frequencies.

GPS Control Segment: The *Control* Segment has five monitor stations, three of which have uplink capabilities. The monitor stations use a GPS receiver to track all satellites in view passively and thus accumulate ranging data from the satellite signals. The information from the monitor stations is processed at the Master Control Station (MCS) to determine satellite orbits and to update the navigation message of each satellite. This updated information is transmitted to the satellites via the ground antennas, which are also used for transmitting and receiving satellite control information.

GPS User Segment: The *User* segment consists of an antenna and receiver processors that provide positions, velocity and precise timing to the respective user. Computing the user's positional information typically requires simultaneous solution of the following four nonlinear position equations [9]:

$$(x_1 - u_x)^2 + (y_1 - u_y)^2 + (z_1 - u_z)^2 = (R_1 - C_B)^2$$
$$(x_2 - u_x)^2 + (y_2 - u_y)^2 + (z_2 - u_z)^2 = (R_2 - C_B)^2$$
$$(x_3 - u_x)^2 + (y_3 - u_y)^2 + (z_3 - u_z)^2 = (R_3 - C_B)^2$$
$$(x_4 - u_x)^2 + (y_4 - u_y)^2 + (z_4 - u_z)^2 = (R_4 - C_B)^2$$

where the pseudo range, $R_{i=1,2,3,4}$ to each satellite is defined as $R_i = C\Delta t$ and

C = speed of light

$\Delta t_{i=1,2,3,4}$ = transmission times to i-th satellite

$x_{i=1,2,3,4}$, $y_{i=1,2,3,4}$, $z_{i=1,2,3,4}$ are respective i-th satellite positions

u_X, u_Y, u_Z is the user position the GPS user equipment is solving numerically and recursively

C_B = the user clock bias (user equipment solves)

Normally the user equipment needs to acquire and maintain lock on four satellites in order to compute a 3-D position fix [28] and the clock bias C_B. The GPS pseudorange between the user and each satellite is computed based on knowledge of time (the master GPS clock) and the unique signal format which is broadcast by each satellite. Once the four pseudo-ranges are known, a recursive algorithm is solved to compute the user's position [28]. Accuracy: Stand-alone (no-aiding) GPS is typically 16 meters (military) and 100 meters (commercial) spherical error probable (SEP). See [9] for further references.

Radar Altimeter: A radar altimeter provides measurement of absolute clearance over all types of terrain [17]. System operation is based on the precise measurement of the time required for an electromagnetic energy pulse to travel from the aircraft to the terrain below and to return. Radar altimeters are normally all-weather devices. Performance specifications (3-σ) are typically $\pm$ [3ft + 3% of altitude range], with $\pm$ 30° pitch and $\pm$ 45° roll maneuverability at above ground level (AGL) heights, which typically vary from 0 feet to 10,000 feet.

Instrument Landing System (ILS) Precision Approach: An *instrument approach*, by definition [21], is the process of making an approach to a landing by the use of navigation instruments without dependence upon direct visual reference to the terrain. The *Instrument Landing System* (ILS) is designed to provide an approach path for exact alignment and descent of an aircraft on final approach to a runway [8]. The ground equipment consists of two highly directional transmitting systems, and along the approach, three (or fewer) marker beacons. The directional transmitters are known as the localizer and glide slope transmitters.

The *localizer* transmitter emits signals which provide the pilot with course guidance to the runway centerline in the horizontal plane. The ultra high frequency *glide slope* transmitter radiates its signals primarily in the direction of the localizer front course, i.e., so as to measure angular vertical displacement from the desired glide path, as seen from the side. A *marker beacon* light and (or) aural tone may be included in the cockpit display to indicate aircraft position along the localizer [8].

Aircraft Precision Landing: Formally defined by the Federal Aviation Administration (FAA) in [11] as Category I, II or III precision approach. See Table 1 [23]:

Precision Approach Parameters (in feet, all 1-sigma values)		
Category	Azimuth	Elevation
I	+/- 28.1	+/- 6.8
II	+/- 8.6	+/- 2.8
III	+/- 6.8	+/- 1.0

Table 1. Precision Approach Accuracy Requirements at Decision Heights

Microwave Landing System (MLS): Proposed land-based replacement navigation aide for the ILS [23,27].

Kalman Filter: A recursive computer algorithm that uses sampled-data measurements to produce optimal estimates of states of a dynamic system, under the assumptions of *linear* system models and white Gaussian noise models [22].

Extended Kalman Filter (EKF): Unfortunately, not all problems are adequately described with linear systems driven by white Gaussian noise. In many cases, the most appropriate model is nonlinear. The navigation problem at hand falls squarely into the nonlinear category. The EKF allows for relinearizing about newly declared nominals at each sample time, to enhance the adequacy of a linearization process and thus the resulting filter performance. The extended Kalman filter equations are summarized below. The reader is referred to [26] for details regarding their derivation.

Suppose that the nonlinear system may be described by [26]:

$$\dot{\mathbf{x}}(t) = \mathbf{f}[\mathbf{x}(t), \mathbf{u}(t), t] + \mathbf{G}(t)\mathbf{w}(t)$$

In this case, the state dynamics vector, $\mathbf{f}[\cdot,\cdot,\cdot]$, is a nonlinear function of the state vector $\mathbf{x}(\cdot)$, time t, and the control input (assumed to be zero in this research). The white Gaussian noise $\mathbf{w}(t)$ has statistics $E\{\mathbf{w}(t)\} = \mathbf{0}$ and $E\{\mathbf{w}(t)\mathbf{w}^T(t+\tau)\} = \mathbf{Q}(t)\delta(\tau)$, and it still enters the dynamics model linearly. In addition, the measurement equation may also be a nonlinear function of the state vector and time:

$$\mathbf{z}(t_i) = \mathbf{h}[\mathbf{x}(t_i), t_i] + \mathbf{v}(t_i)$$

The noise vector $\mathbf{v}$ is again *zero-mean*, white and Gaussian, entering the measurement equation linearly, and its covariance is described by

$$E\{\mathbf{v}(t_i)\mathbf{v}^T(t_j)\} = \begin{cases} \mathbf{R}(t_i) \; for \; t_i = t_j \\ \mathbf{0} \; for \; t_i \neq t_j \end{cases}$$

Measurements are incorporated into the extended Kalman filter via the following set of equations [26]:

$$\mathbf{K}(t_i) = \mathbf{P}(t_i^-)\mathbf{H}^T[t_i;\hat{\mathbf{x}}(t_i^-)]\left\{\mathbf{H}[t_i;\hat{\mathbf{x}}(t_i^-)]\mathbf{P}(t_i^-)\mathbf{H}^T[t_i;\hat{\mathbf{x}}(t_i^-)] + \mathbf{R}(t_i)\right\}^{-1}$$

$$\hat{\mathbf{x}}(t_i^+) = \hat{\mathbf{x}}(t_i^-) + \mathbf{K}(t_i)\left\{\mathbf{z}_i - \mathbf{h}[\hat{\mathbf{x}}(t_i^-); t_i]\right\}$$

$$\mathbf{P}(t_i^+) = \mathbf{P}(t_i^-) - \mathbf{K}(t_i)\mathbf{H}[t_i;\hat{\mathbf{x}}(t_i^-)]\mathbf{P}(t_i^-)$$

where

$$\mathbf{H}[t_i;\hat{\mathbf{x}}(t_i^-)] = \left.\frac{\partial \mathbf{h}[\mathbf{x}, t_i]}{\partial \mathbf{x}}\right|_{\mathbf{x} = \hat{\mathbf{x}}(t_i^-)}$$

The state estimate and covariance are propagated from t_i to t_{i+1} by integrating the following equations [26]:

$$\dot{\hat{\mathbf{x}}}(t/t_i) = \mathbf{f}[\hat{\mathbf{x}}(t/t_i), \mathbf{u}(t), t]$$

$$\dot{\mathbf{P}}(t/t_i) = \mathbf{F}[t;\hat{\mathbf{x}}(t/t_i)]\mathbf{P}(t/t_i) + \mathbf{P}(t/t_i)\mathbf{F}^T[t;\hat{\mathbf{x}}(t/t_i)] + \mathbf{G}(t)\mathbf{Q}(t)\mathbf{G}^T(t)$$

where

$$\mathbf{F}[t;\hat{\mathbf{x}}(t/t_i)] = \left.\frac{\partial \mathbf{f}[\mathbf{x}(t), t_i]}{\partial \mathbf{x}}\right|_{\mathbf{x} = \hat{\mathbf{x}}(t/t_i)}$$

and the initial conditions are:

$$\hat{\mathbf{x}}(t_i / t_i) = \hat{\mathbf{x}}(t_i^+)$$

$$\mathbf{P}(t_i / t_i) = \mathbf{P}(t_i^+)$$

The equations shown above for the extended Kalman filter are programmed into the MSOFE shell [31] for the problem defined by this paper. It is the fact that the extended Kalman filter is relinearized about each successive estimate of the state $\hat{\mathbf{x}}(t)$ which "enhances the validity of the assumption that deviations from the reference (nominal) trajectory are small enough to allow linear perturbation techniques to be employed" [26].

5. Landing System Computer Model

The Landing System Model (LSM) depicted in Figure 1 and Figure 2 illustrates the overall goal: GPS and radar altimeter measurement information must be fed into an extended Kalman filter to determine the errors, δx, in the INS. Our extended Kalman filter *estimates* the true error, δx, of the INS with an output we note as "$\delta\hat{x}$". Once the best estimates, $\delta\hat{x}$, are determined by our extended Kalman filter, we then subtract them (in a feed-forward approach) from the output of the simulated INS blackbox. The feedforward approach is utilized in this project due to current Federal Aviation Administration (FAA) restrictions on providing

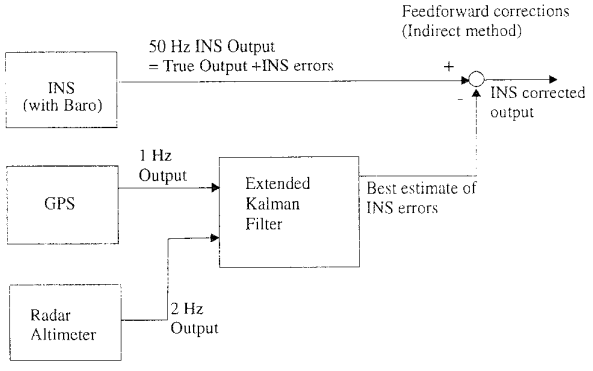

Figure 1. Overall Landing System Model (LSM) Description

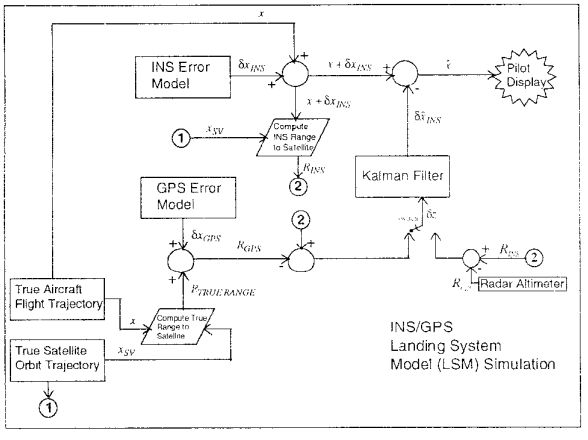

Figure 2. LSM Truth and Filter Model Block Diagram

"feedback" to the INS. The computer modeling of the LSM is divided into two portions, the truth model and the filter model. The truth model represents computer-generated simulation of error characteristics of avionics "black-boxes" and environment, that would normally be found in the real world. Because the information and data presented in this project was accomplished entirely through computer simulation, the truth model will simulate the errors in true avionics hardware (INS, GPS, Baro, Radar Altimeter) black-boxes. The truth model generates the measurement updates for the LSM filter, the true flight profile of the aircraft and a state variable baseline for evaluating filter performance [29]. The truth model consists of 69 error states about their nominal values. The filter model represents the LSM in its functional form, which is the basis of the filter which could be hosted on-board an aircraft computer. The LSM filter model is a 13-state model that has been developed through order reduction of the truth model of [29]. The author's approach was to begin the filter state building using the fewest possible states that would meet precision approach landing requirements. The 13-state LSM was chosen as a first-cut model. An advantage of using only 13 states is that it is not over-burdening to current state-of-the-art aircraft host computers, keeping practicality and dollar affordability in mind. The block diagram, Figure 2 explains how the filter and truth models interact in the MSOFE computer simulation. PROFGEN [30] provides a simulated flight profile and the U.S. Coast Guard GPS Bulletin Board Service (BBS) [13] provides true SV ephemeris data for any SV.

Use of the "real-world" ephemeris replaced the prior FORTRAN ORBIT functions used by past researchers at AFIT [2,29,36]. The best four SV were chosen by using System Effectiveness Model (SEM) software [10] and selecting the best (lowest) position dilution of precision (PDOP). With this information, the truth model is able to simulate a real world INS navigation solution, $x + \delta x_{INS}$, and generate the real world GPS and radar altimeter measurements, R_{GPS} and R_{ralt} respectively. The LSM filter in Figure 2 is represented by the Kalman filter block. The corrections from the LSM filter are subtracted from the INS navigation solution to generate the best possible navigation solution available, $\hat{x} = x + \delta x_{INS} - \delta\hat{x}_{INS}$ [29]. The switch in Figure 2 does not imply "either/or", instead it implies use of radar altimeter measurements as well as GPS receiver outputs can be used. Now that the MSOFE implementation of the LSM filter has been explained, the truth and filter models for the GPS, radar altimeter and the INS subsystems will be described.

6. Models

The LSM simulation is composed of the truth model and filter, both in *error state* form. The LSM truth model represents the real world. It consists of a total of 69 error states. The LSM filter model is derived from the LSM truth model through error state order-reduction. Since the LSM truth and filter models utilize error states, it is necessary to develop difference measurement update equations for all the measurements. This will now be done briefly; for a more detailed explanation, see [15].

INS Truth Model: The INS truth model (39 error-states) represent a strapped-down wander azimuth system that senses aircraft motion via gyros and accelerometers and is used as the primary source for navigation [29]. The INS model has been derived from a medium accuracy RLG INS 93-state model [1,24], thus the INS error state

truth model is a 39-state reduced-order version of the 93-state model [24]. The order reduction was performed according to [29]. It was an objective in this project to compare a medium accuracy INS (0.4 nm/hr) with a lower quality inertial navigation systems in the range of 2 to 4 nm/hr. The choice of error state modification to the existing NRS INS model [29,32] to create the other two models was based in part from personal conversations with [19]. Modifications to the system covariance matrices for each respective INS are shown in [15]. Only random constant shaping filter states were changed (not the 1st order Gauss-Markov drift states, etc.). The CEP curves for one hour of operation of the three inertial navigation systems created in this project are shown in [15].

INS Filter Model: The INS filter model retains the essential states from the 39-state truth model. It consists of 11 dominant error states from the 39 state truth model. The final INS filter dynamics submatrix, **F**, as well as process noise strength **Q** and measurement noise covariance **R,** can be found in [15].

INS Measurement Model: The two measurements other than GPS that are used to update the filter are the barometric altimeter and the radar altimeter. The barometric altimeter signal is used to correct for inherent instabilities of the vertical channel in the filter. The radar altimeter is used during landing approaches when altitudes are below 3000 feet above ground level (AGL). The barometric altimeter measurement equation is based on the difference between the INS-predicted altitude, Alt_{INS} and the barometric altimeter-predicted altitude Alt_{Bar}:

$$\delta z_{Alt} = Alt_{INS} - Alt_{Bar}$$

Therefore it is necessary to develop the two separate measurement signals that will be differenced to attain the proper measurement update for the error state filter [29]. The INS-predicted altitude is the sum of the true altitude, h_t, and the INS error in vehicle altitude above the reference ellipsoid, δh. The barometric altimeter reading is modeled as the sum of the true altitude, h_t, the total time-correlated error in the barometric altimeter, δh_B, and a random measurement noise, v. Subtracting the INS-predicted altitude from the barometric altimeter altitude we compute:

$$\begin{aligned}\delta z_{Alt} &= Alt_{INS} - Alt_{Bar} \\ &= [h_t + \delta h] - [h_t + \delta h_B - v] \\ &= \delta h - \delta h_B + v\end{aligned}$$

Note that, since v is assumed *zero* mean, white gaussian noise, statistically speaking, one can choose v with either a plus "+" or minus "-" coefficient. The author chooses the coefficient carefully so that the end result shows a plus "+v" sign.

As a "first-cut" model of the radar altimeter, the measurement equation is based on the difference between the INS predicted altitude, Alt_{INS} and the radar altimeter predicted altitude, Alt_{Ralt}:

$$\delta z_{Alt} = Alt_{INS} - Alt_{Bar}$$

Note that the errors in the radar altimeter are represented totally as white noise, with no time-correlated component at all. Though admittedly only a first-cut model, it should be sufficient to demonstrate important performance trends.

The radar altimeter measurement noise variance, R_{Filter} or R_{True}, is a function of aircraft altitude above ground level (AGL). The filter model noise variance from [17]:

$$R_{Filter} = \left\{[0.01]^2 * [Radar\ Altitude_{True(AGL)}]^2\right\} + 0.25_{Bias}$$

and the truth model noise variance is the same:

$$R_{Truth} = \left\{[0.01]^2 * [Radar\ Altitude_{True(AGL)}]^2\right\} + 0.25_{Bias}$$

Note that R_{Filter} and R_{Truth} are both time-varying rather than constant, due to the altitude dependency.

GPS Model: The GPS navigation system used is based on electromagnetic signals transmitted from orbiting GPS satellites. This model has been developed throughout research at AFIT, and many of its fundamental concepts are addressed in a variety of sources [25,32,35,36]. GPS generates navigation information by acquiring the range to multiple satellites of known position, called "*pseudoranges*". The navigation information passed to the LSM filter is the respective range and ephemeris data position to each of four satellites [25,29]. The GPS truth model consists of 30 error states and the GPS filter model consists of only the following two error states (user clock bias and drift):

$$\begin{Bmatrix}\delta\dot{R}_{clk_u} \\ \delta\dot{D}_{clk_u}\end{Bmatrix} = \begin{bmatrix}0 & 1 \\ 0 & 0\end{bmatrix}\begin{Bmatrix}\delta R_{clk_u} \\ \delta D_{clk_u}\end{Bmatrix} + \begin{Bmatrix}w_{R_{clk}} \\ w_{R_{clk}}\end{Bmatrix}$$

Various research efforts have shown that two states provide a sufficient model for GPS [29,32,33]. The primary argument is that the errors modeled by the other 28 states are small when compared to the two states common to all SV's. By adding dynamics driving noise, of strength Q, and re-tuning the filter, the overall performance of the LSM can be maintained with the significantly reduced-order model shown above.

GPS Measurement Model: There are four GPS scalar measurement updates, one from each of the satellite range signals received by the LSM filter. These measurement updates are once again *difference* measurements. The GPS difference measurement is formed by taking the difference of the INS-calculated pseudorange, R_{INS} and measured pseudorange, R_{GPS}.

$$\delta z_{GPS} = R_{INS} - R_{GPS}$$

The real pseudorange, R_{GPS} is the sum of the true range form the user to the satellite plus all the errors in the pseudorange signal propagation.

$$R_{GPS} = R_t + \delta R_{cloop} + \delta R_{trop} + \delta R_{ion} + \delta R_{Sclk} + \delta R_{Uclk} - v$$

where

R_{GPS}	=	GPS pseudorange measurement, from SV to user
R_t	=	true range, from SV to user
δR_{cloop}	=	range error due to code loop error
R_{trop}	=	range error due to tropospheric delay

δR_{ion} = range error due to ionospheric delay

δR_{Sclk} = range error due to SV clock error

δR_{Uclk} = range error due to use clock error

v = zero-mean white Gaussian measurement noise

The second source of a range measurement is the INS itself, R_{INS} [29]. R_{INS} is the difference between the LSM-calculated position, X_U and the satellite position from the ephemeris data X_S.

This difference vector is represented below in the ECEF frame:

$$R_{INS} = |X_U - X_S| = \left| \begin{Bmatrix} x_U \\ y_U \\ z_U \end{Bmatrix}^e - \begin{Bmatrix} x_S \\ y_S \\ z_S \end{Bmatrix}^e \right|$$

the GPS pseudorange truth model *difference* measurement is given as the truncated Taylor series:

$$\begin{aligned} \delta z_{GPS_i} &= R_{INS} - R_{GPS} \\ &= -\left[\frac{x_S - x_U}{|R_{INS}|}\right]\cdot\delta x_U - \left[\frac{y_S - y_U}{|R_{INS}|}\right]\cdot\delta y_U - \left[\frac{z_S - z_U}{|R_{INS}|}\right]\cdot\delta z_U \\ &+ \left[\frac{x_S - x_U}{|R_{INS}|}\right]\cdot\delta x_S + \left[\frac{y_S - y_U}{|R_{INS}|}\right]\cdot\delta y_S + \left[\frac{z_S - z_U}{|R_{INS}|}\right]\cdot\delta z_S \\ &- [1]\delta R_{cloop} - [1]\delta R_{trop} - [1]\delta R_{ion} \\ &- [1]\delta R_{Sclk} - [1]\delta R_{Uclk} + v \end{aligned}$$

The filter model measurement equation can therefore be written as:

$$\begin{aligned} \delta z_{GPS_i} &= R_{INS} - R_{GPS} \\ &= -\left[\frac{x_S - x_U}{|R_{INS}|}\right]\cdot\delta x_U - \left[\frac{y_S - y_U}{|R_{INS}|}\right]\cdot\delta y_U - \left[\frac{z_S - z_U}{|R_{INS}|}\right]\cdot\delta z_U \\ &- [1]\delta R_{Uclk} + v \end{aligned}$$

The filter measurement noise variance, R, will be tuned to attain adequate performance despite (1) the reduction in order from the truth model and (2) the Taylor series approximation. The measurement noise variances for both the filter and the truth model equations are provided in [15].

7. Results

The sixteen integration cases shown in Table 2 were performed. All cases use the Tanker (KC-135) flight profile of Section 5 and the P-Code receiver always uses four SVs overhead. Cases I - VI show how the additional radar altimeter measurements can aid three different INS's using baro altimeter and a P-Code GPS receiver. Cases VII - IX show how use of a single pseudolite measurement in close proximity to a runway can aid three different INS's using baro altimeter and P-Code GPS aiding. Cases X - XII show the performance enhancements of using a single pseudolite measurement and radar altimeter measurements. It should be remembered that by no means is the location of the single pseudolite "optimal". No real criterion was used when selecting the pseudolite location. The results of Cases X - XII can be compared with Cases (I, III, V) - no radar altimeter or pseudolite, Cases (II, IV, VI) - just

Case I	Case II	Case III	Case IV	Case V	Case VI
Baro Altimeter	Baro Altimeter	Baro Altimeter	Baro Altimeter	Baro Altimeter	Baro Altimeter
0.4 nm/hr CEP INS	0.4 nm/hr CEP INS	2.0 nm/hr CEP INS	2.0 nm/hr CEP INS	4.0 nm/hr CEP INS	4.0 nm/hr CEP INS
P-Code GPS	P-Code GPS	P-Code GPS	P-Code GPS	P-Code GPS	P-Code GPS
--	Radar Altimeter	-----	Radar Altimeter	-----	Radar Altimeter

Case VII	Case VIII	Case IX	Case X	Case XI	Case XII
Baro Altimeter	Baro Altimeter	Baro Altimeter	Baro Altimeter	Baro Altimeter	Baro Altimeter
0.4 nm/hr CEP INS	2.0 nm/hr CEP INS	4.0 nm/hr CEP INS	0.4 nm/hr CEP INS	2.0 nm/hr CEP INS	4.0 nm/hr CEP INS
P-Code GPS	P-Code GPS	P-Code GPS	P-Code GPS	P-Code GPS	P-Code GPS
Pseudolite	Pseudolite	Pseudolite	Radar Altimeter and Pseudolite	Radar Altimeter and Pseudolite	Radar Altimeter and Pseudolite
No GPS Outage	No GPS Outage	No GPS Outage	No GPS Outage	No GPS Outage	No GPS Outage

Case XIII	Case XIV	Case XV	Case XVI
Barometric Altimeter	Barometric Altimeter	Barometric Altimeter	Barometric Altimeter
0.4 nm/hr CEP INS	2.0 nm/hr CEP INS	4.0 nm/hr CEP INS	4.0 nm/hr CEP INS
P-Code GPS	P-Code GPS	P-Code GPS	P-Code GPS
None	None	None	Radar Altimeter
Single GPS Outage	Single GPS Outage	Single GPS Outage	Double GPS Outages

Table 2. Case I-XVI Integration Comparisons

radar altimeter, and Cases (VII, VIII, IX) - just pseudolite, to see the additional benefit of each measurement source. Case XIII - XV shows simply a single GPS outage, with the 0.4/2/4 nm/hr INSs. Use of the radar altimeter occurs during final approach. Case XVI shows a double GPS outage; where use of radar altimeter occurs during the aircraft landing. Only the 4 nm/hr INS is evaluated for this special case. Also, all results will be compared with Table 1, illustrating landing performance 1σ requirements at respective decision heights. Tabular listings of the truth and filter models are presented in [15]. Also a top and side view of the tanker aircraft precision approach can be found in [15].

The following four tables show the time-averaged rms errors for the various cases. In tables 3 - 5, the results from three different INS's are averaged, since they were virtually indistinguishable.

Error State	Case I, III, V average true error (feet)	Case VII - IX average true error (feet)	% Change in Error
Latitude	8.9	4.6	48.3%
Longitude	9.2	3.9	57.6%
Altitude	15.0	11.8	21.3%
Clock Bias	9.0	4.9	45.6%

Table 3. Averaged True Error Reduction Using a Single Pseudolite

Error State	Case II, IV, VI average true error (feet)	Case X - XII average true error (feet)	% Change in Error
Latitude	8.8	4.4	50.0%
Longitude	9.2	3.3	64.1
Altitude	2.6	2.4	7.7%
Clock Bias	7.5	4	46.7%

Table 4. Averaged True Error Reduction, Case II-IV-VI vs. Case X-XI-XII

Error State	Case VII, VIII, IX average true error (feet)	Case X - XII average true error (feet)	% Change in Error
Latitude	4.6	4.4	4.4%
Longitude	3.9	3.3	15.4%
Altitude	11.8	2.4	79.7%
Clock Bias	4.9	4	18.4%

Table 5. Averaged True Error Reduction, Case VII-VIII-IX vs. Case X-XI-XII

Error State	Case VI average true error (feet)	Case XVI average true error (feet)	% Change in Error
Latitude	8.8	9.2	4.5%
Longitude	9.4	9.7	3.2%
Altitude	2.3	3.6	56.5%
Clock Bias	6.0	6.1	1.7%

Table 6. Averaged True Error % Change, Case VI vs. Case XVI

Table 7 and 8 summarize all cases that met Table 1 precision approach requirements. Note that no Category III precision approach was deemed possible by any Case number in this project.

Precision Approach Category	Case I	Case II	Case III	Case IV	Case V	Case VI	Case VII	Case VIII
I	No	Yes	No	Yes	No	Yes	No	No
II	---	---	---	---	---	---	---	---

Table 7. Summary of Cases I - VIII: Precision Approach Requirements Met

Precision Approach Category	Case IX	Case X	Case XI	Case XII	Case XIII	Case XIV	Case XV	Case XVI
I	No	---	---	---	No	No	No	Yes
II	---	Yes	Yes	Yes	---	---	---	---

Table 8. Summary of Cases IX - XVI: Precision Approach Requirements Met

8. Summary

Very few "integrated" GPS/INS studies have been accomplished with respect to implementing precision landing approaches. Instead, the majority of research efforts have explored stand-alone GPS receiver technology. Instead of stand-alone GPS techniques, this project *integrated* the GPS with an INS/Baro altimeter system and a radar altimeter using an extended Kalman filter to meet FAA Category I and II precision approach *accuracy* requirements.

In order to accomplish project goals, this project concentrated on setting up reliable models for three different classes of INS (0.4, 2.0 and 4.0 nm/hr (CEP) INS systems), GPS (4 channel receiver, 5m vertical and 4m horizontal precision, 1σ), Baro Altimeter (50 - 150 ft, 1σ), and Radar altimeter (1% of altitude + "floor" value, 1σ). This project also developed a generic precision approach flight profile (using PROFGEN [30]) that encompassed a majority of aircraft types. Lastly, this project utilized a single ground-based SV (pseudolite) and available true post-processed ephemeris data [6,13], instead of prior *simulated* ephemeris data used at AFIT [2,16,29,32,36]. Once all the above elements were in place, the Multimode Simulation for Optimal Filter Evaluation (MSOFE) [31] was utilized to perform extended Kalman Filter integration analysis.

Use of an existing 0.4 nm/hr, 2.0 nm/hr and lower quality 4.0 nm/hr INS, when properly integrated with a 4-channel P-code GPS receiver and radar altimeter, can meet the FAA Category I precision approach. Use of an existing 0.4 nm/hr, 2.0 nm/hr and lower quality 4.0 nm/hr INS, when properly integrated with a 5-channel P-code GPS receiver (one channel using a ground based pseudolite) and radar altimeter, can meet the FAA Category II precision approach. These conclusions are made based on mainly four main assumptions:

1. Error models used in this simulation are realistic to the respective real-world black box output errors.
2. No radar altimeter measurement outages occur during the landing approach.
3. When radar altimeter measurements are available, the earth's surface will be modeled as flat and referenced approximately to the INS-indicated altitude (referenced to WGS-84 ellipsoid).
4. When use of the single pseudolite information is used, ionospheric, tropospheric, pseudolite position, pseudolite clock and multipath errors are negligible.

In order to meet a Category III approach, more precise measurements must be made available. Recommendations are as follows:

1. Make use of the 30 centimeter (1-σ) accuracy of *carrier-phase* GPS signals, now readily available in commercial receivers. The carrier-phase information can be used for positional information as well as heading information (using multiple antennas) [39]. Decide whether one's algorithm will also handle "integer ambiguity" techniques, or assume no cycle slips. See [3,16] for more information regarding carrier-phase integer ambiguity and cycle slips.
2. Use Differential GPS measurements at all times for North America (assume wide-area differential will be available). The models for filter design and for performance evaluation must make the distinction of representing a C/A or P-code receiver using differential corrections.
3. Maintain use of at least one pseudolite along the flight path. In fact, current flight testing is showing that use of two pseudolites optimally placed along the approach path is recommended [3].
4. Use, as a minimum, six (6) independent SV measurements (though, for any given time, use of *all* in-view SVs is preferred) rather than the current (archaic) military standard of four SVs (to minimize geometric dilution of precision (GDOP errors). (This project only used cases where 4 SV or 5 SV were used at one time).
5. Obtain and use published geographic data of respective airport terrain, so as to reference the radar altimeter outputs to WGS-84 ellipsoid (to match the INS positional outputs).
6. Use single filter (then continue analysis with small, non-computer-burdening multiple filters) and perform residual monitoring for use as a fault detection and isolation algorithm for GPS Space Segment system errors, to compensate for deliberate and non-deliberate jamming and spoofing of the SV signals. Fault detection must notify the pilot of a possible degraded navigation solution in less than 2 seconds, while minimizing false alarms.
7. Explore utilizing dynamic filter tuning procedures along the approach path when using pseudolites (e.g., at a given runway, multipath errors may be excessive; "R" tuning of the respective measurement may be necessary).

9. Bibliography

1. Aeronautical Systems Division, AFSC. *Specification for USAF Standard Form, Fit and Function (F3) Medium Accuracy Inertial*

Navigation Unit, F-16 Aircraft Application. SNU84-1/F-16, Revision A, Change Notice 1, Wright-Patterson AFB, OH, 20 Aug 1991.

2. Bagley, Daniel T. *GPS/INS Integration for Improved Aircraft Attitude Estimates.* MS Thesis, AFIT/GE/ENG/91D-04. School of Engineering, Air Force Institute of Technology, Wright-Patterson AFB OH, December 1992 (AD-A243947).

3. Bohenek, Brian J. *The Enhanced Performance of an Integrated Navigation System in a Highly Dynamic Environment.* MS Thesis, AFIT/GE/ENG/94D-01. School of Engineering, Air Force Institute of Technology, Wright-Patterson AFB, OH, December 1994.

4. Britting, Kenneth R. *Inertial Navigation Systems Analysis.* New York: Wiley-Interscience, 1971.

5. Cohen, Clark. Avionics Research Engineer. Department of Aeronautics and Astronautics, Stanford University. Telephone Interview. November 1994.

6. Defense Mapping Agency. Department of Defense World Geodetic System 1984. DMA Technical Report, DMA TR 8350.2. 30 Sep 1987.

7. Department of Defense. *Flight Information Publication. (Terminal) Low Altitude United States Airport Diagrams. Instrument Approach Procedures.* Volume 8, Pages 339-340. 28 April 94.

8. Department of the Air Force. *Flying Training: Instrument Flying.* AFM 51-37. Washington: HQ USAF, 15 July 1986.

9. Department of the Air Force. *NAVSTAR GPS USER EQUIPMENT.* MZI0298.001, US Air Force Space Systems Division, NAVSTAR-GPS Joint Program Office, Los Angeles, CA. February 1991.

10. Department of the Air Force. *Single-Location User, System Effectiveness Model Demonstration Software (Version 3.6) Reference Manual,* Joint Program Office, Directorate of Systems Engineering, Los Angeles CA. March 1990.

11. Department of Transportation. *FAR-AIM (Federal Aviation Regulations and Airman's Information Manual) Part 1,* Aviation Supplies & Academics, Inc., Renton, WA., 1993.

12. Department of Transportation. *Federal Aviation Administration (FAA) Satellite Navigation Program Master Plan, ARD-70. FY 93-98,* Projected Civil Aviation GPS Operational Implementation Schedule, Washington, D.C.: Federal Aviation Administration, 15 Feb 93.

13. Department of Transportation. *Global Positioning System Information Center (GPSIC) Users Manual.* Bulletin Board Phone Number: (703) 313-5910. United States Coast Guard, Alexandria, VA, September 1992.

14. Farrel, James L. *Integrated Aircraft Navigation.* New York: Academic Press, 1976.

15. Gray, Robert A. *An Integrated GPS/INS/BARO and Radar Altimeter System for Aircraft Precision Approach Landings.* MS Thesis, AFIT/GE/ENG/94D-13. School of Engineering, Air Force Institute of Technology, Wright-Patterson AFB OH, December 1994.

16. Hansen, Neil P. *Incorporation of Carrier-Phase Global Positioning System Measurements into the Navigation Reference System for Improved Performance.* MS Thesis, AFIT/GE/ENG/93D-40. School of Engineering, Air Force Institute of Technology, Wright-Patterson AFB OH, December 1993 (AD-A274136).

17. Honeywell Military Avionics Division. *Honeywell AN/APN-194 Pulse Radar Altimeter System.* Honeywell Technical Description, Minneapolis: June 1989.

18. Honeywell Military Avionics Division. *Ring Laser Gyro.* Honeywell LaserReady News, Vol 90, Number 2. 1990.

19. Ignagni, Mario. Avionics Engineer, Honeywell Commercial Avionics, Minneapolis, MN. Personal Correspondence. May 1994.

20. Inertial Navigation System, STM 16-829 Vol I & II, *F-16 Block 40 Configuration, Training Manual,* General Dynamics, FortWorth, TX: 10 Jun 90.

21. Institute of Electrical and Electronics Engineers. *IEEE Standard Dictionary of Electrical and Electronics Terms.* IEEE Std 100-1972. New York.

22. Kalman, R.E., "A New Approach to Linear Filtering and Prediction Problems," *Transactions ASME, Series D: Journal of Basic Engineering,* 1960.

23. Kelly, Robert, and Jerry Davis, *RNP Tunnel Concept for Precision Approach and Landing,* RTCA, Inc., SC159 Working Group 4, MT/140, January 1993.

24. Knudsen, L. *Performance Accuracy (Truth Model/Error Budget) Analysis for the LN-93 Inertial Navigation Unit.* Technical Report, Litton Guidance and Control Systems, Woodland Hills, CA: January 1985. DID No. DI-S-21433 B/T:CDRL No. 1002.

25. Martin, E.H. "GPS User Equipment Error Models," *The Institute of Navigation, Volume I:*109-118 (1980).

26. Maybeck, Peter S. *Stochastic Models, Estimation, and Control.* Volume 2. New York: Academic Press, Inc., 1982.

27. Meyer-Hilberg, Jochen, and Thomas Jacob. "High Accuracy Navigation and Landing System Using GPS/IMU System Integration," *IEEE Trans. Position Location and Navigation Symposium, Las Vegas:* 0-7803-1435-2/94, 298-305 (April 11-15, 1994).

28. Milliken, R.J., and C.J. Zoller. "Principle of Operation of NAVSTAR and System Characteristics," *Global Positioning System,* The Institute of Navigation, Volume I. Alexandria, VA 22314, 1980.

29. Mosle, William B. *Detection, Isolation, and Recovery of Failures in an Integrated Navigation System.* MS Thesis, AFIT/GE/ENG/93D-28. School of Engineering, Air Force Institute of Technology, Wright-Patterson AFB OH, December 1993 (AD-A274056).

30. Musick, Stanton H. *PROFGEN - A Computer Program for Generating Flight Profiles.* Technical Report, Air Force Avionics Laboratory, WPAFB, OH, November 1976. AFAL-TR-76-247, DTIC ADA034993.

31. Musick, Stanton H., and Neil Carlson. *User's Manual for a Multimode Simulation for Optimal Filter Evaluation (MSOFE).* AFWAL-TR-88-1138, Wright-Patterson AFB OH: A.F. Avionics Laboratory, AFWAL/AARN-2, April 1990.

32. Negast, William Joseph. *Incorporation of Differential Global Positioning System Measurements Using an Extended Kalman Filter for Improved Reference System Performance.* MS Thesis, AFIT/GE/ENG/91D-41. School of Engineering, Air Force Institute of Technology, Wright-Patterson AFB OH, December 1991 (AD-A243742).

33. Riggins, Lt Col Robert N., and Capt Ron Delap, . Assistant Professors of Electrical Engineering, Air Force Institute of Technology, Wright-Patterson AFB, OH. Course Notes EENG 534/635. 1993-94.

34. Savage, Paul G. "Strapdown Sensors," *AGARD Lecture Series No. 95* (June 1978).

35. Snodgrass, Faron Britt. *Continued Development and Analysis of a New Extended Kalman Filter for the Completely Integrated Reference Instrumentation System (CIRIS).* MS Thesis, AFIT/GE/ENG/90M-5. School of Engineering, Air Force Institute of Technology (AU), Wright-Patterson AFB OH, March 1990 (AD-A220106).

36. Solomon, Capt Joseph , Research Scientist, Wright Laboratories, Wright-Patterson AFB, OH. Personal Interviews. April 1994 - November 1994.

37. Stacey, Richard D. *A Navigation Reference System (NRS) Using Global Positioning System (GPS) and Transponder Aiding.* MS Thesis, AFIT/GE/ENG/91M-04. School of Engineering, Air Force Institute of Technology, Wright-Patterson AFB OH, March 1991 (AD-A238890).

38. The MathWorks, Inc., 21 Elliot Street, Natick, MA 01760. *Matlab.* December 1992. Version 4.0a.

39. van Graas, Frank. Associate Professor of Electrical Engineering, Ohio University. Telephone Conversations. September 1994.